Title

DNA Nanotweezers and Graphene Transistor Enable Label-Free Genotyping

Journal

Advanced Materials, 30(34)

ISSN

0935-9648

Authors

Hwang, Michael T
Wang, Zejun
Ping, Jinglei
et al.

Publication Date

2018-08-01

DOI

10.1002/adma.201802440

Peer reviewed

Published in final edited form as:

Adv Mater. ; : e1802440. doi:10.1002/adma.201802440.

DNA Nano-tweezers and Graphene Transistor Enable Label-free Genotyping

Michael T. Hwang,
Materials Science and Engineering Program, University of California San Diego, 9500 Gilman Drive, La Jolla, CA 92093, USA

Zejun Wang,
Division of Physical Biology and Bioimaging Center, Shanghai Synchrotron Radiation Facility, CAS Key Laboratory of Interfacial Physics and Technology, Shanghai Institute of Applied Physics, Chinese Academy of Sciences, University of Chinese Academy of Sciences, Shanghai 201800, China

Jinglei Ping,
Department of Physics and Astronomy, University of Pennsylvania, Philadelphia 19104, United States

Deependra Kumar Ban,
Department of Mechanical and Aerospace Engineering, University of California San Diego, 9500 Gilman Drive, La Jolla, CA 92093, USA

Zi Chao Shiah,
Department of Electrical and Computer Engineering, University of California San Diego, 9500 Gilman Drive, La Jolla, CA 92093, USA

Leif Antonschmidt,
NMR Based Structural Biology, Max Planck Institute for Biophysical Chemistry, Am Fassberg 11, 37077 Göttingen, Germany

Joon Lee,
Materials Science and Engineering Program, University of California San Diego, 9500 Gilman Drive, La Jolla, CA 92093, USA

Yushuang Liu,
School of Life Science, Inner Mongolia Agricultural University, 306 Zhaowuda Road, Hohhot 010018, China

Abhijith G. Karkisaval,
Department of Mechanical and Aerospace Engineering, University of California San Diego, 9500 Gilman Drive, La Jolla, CA 92093, USA

A.T. Charlie Johnson [Prof],
Department of Physics and Astronomy, University of Pennsylvania, Philadelphia 19104, United States

M. T. Hwang
Current address: Micro and Nanotechnology Laboratory, University of Illinois Urbana-Champaign, Champaign, IL 61801, USA

Chunhai Fan [Prof],
Division of Physical Biology and Bioimaging Center, Shanghai Synchrotron Radiation Facility, CAS Key Laboratory of Interfacial Physics and Technology, Shanghai Institute of Applied Physics, Chinese Academy of Sciences, University of Chinese Academy of Sciences, Shanghai 201800, China

Gennadi Glinsky [Prof], and
Institute of Engineering in Medicine, University of California San Diego, 9500 Gilman Drive, La Jolla, CA 92093, USA

Ratnesh Lal [Prof]
Materials Science and Engineering Program, University of California San Diego, 9500 Gilman Drive, La Jolla, CA 92093, USA

Department of Mechanical and Aerospace Engineering, University of California San Diego, 9500 Gilman Drive, La Jolla, CA 92093, USA

Department of Bioengineering, University of California San Diego, 9500 Gilman Drive, La Jolla, CA 92093, USA

Abstract

Electronic DNA-biosensor with a single nucleotide resolution capability is highly desirable for personalized medicine. However, existing DNA-biosensors, especially single nucleotide polymorphism (SNP) detection systems have poor sensitivity and specificity and lack real-time wireless data transmission. We have used DNA-tweezers with graphene FET for SNP detection and transmitted data for analysis by wireless. Picomolar sensitivity of quantitative SNP detection was achieved by observing changes in Dirac point shift and resistance change. The use of DNA-tweezers probe with high quality graphene FET significantly improves analytical characteristics of SNP detection by enhancing the sensitivity more than 1,000-fold in comparison to our previous work. The electrical signal resulting from resistance changes triggered by DNA strand-displacement and related changes in the DNA geometry was recorded and transmitted remotely to personal electronics. Practical implementation of this enabling technology will provide cheaper, faster and portable point-of-care molecular health status monitoring and diagnostic devices.

Abstract

Sensing and wireless transmission of genetic mutations with picomolar sensitivity. **Top**: DNA nano tweezers-based sensors of genetic defects. Specific interactions between sensors and mutant nucleic acids release electrons and reduce distance between sensors and graphene surface. **Bottom**: Electric current changes triggered by molecular interactions are captured by graphene FET detector. Signal is transmitted wirelessly to smartphones or smartwatches in real-time.

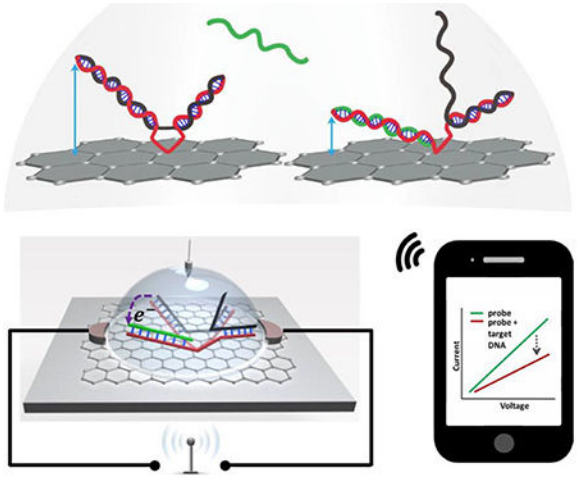

Keywords

graphene FET biosensor; DNA strand displacement; DNA tweezers; electrical wireless biosensor; single nucleotide polymorphism (SNP) detection

The detection and sequencing of DNA and RNA molecules for diagnostics,[1] forensics,[2] and environmental monitoring[3] are of great interest in global personalized medicine. Current DNA and RNA nucleic acids detection methods primarily are not lable-free, they use fluorescent labeling and require sophisticated and lab-based fluorimeters or laser scanners to analyze optical signals. Unfortunately, none of the existing commercially available abovementioned technologies can be developed into portable sensors for early detection of genetic markers for devastating human disorders such as cancer and Alzheimer's disease. Miniaturized chip-based electrical detection of DNA will eliminate the aforementioned limitations and would enable in-field or at home detection of specific DNA sequences and polymorphisms.[4] Significantly, electrical sensing-based methods have successfully lowered the limit of sequence specific DNA detection to the femtomolar level[5, 6] and thus should allow no need for PCR amplification of the genetic materials. A field effect transistor (FET) can be employed as a highly sensitive DNA sensor and can potentially be integrated with other on-chip analytical systems.

Graphene,[7] an atomic-layer of carbon atoms arranged in honeycomb lattice, is ideal to serve as the transducer of a biosensing platform. All charge carriers (holes/electrons) in graphene, confined in a narrow range closed to the surface of graphene, are exposed and thus are ultra susceptive to electrostatic variation in the surrounding environment. Furthermore, FET electrical devices based on graphene have low intrinsic electrical noise. These two combined features make graphene an extremely sensitive material for biosensing applications. Graphene-based detection of macro-sized bacteria has been reported.[8] These bacterial surfaces contain considerably larger electrical charges and hence relatively easier to be detected.

DNA biosensors using graphene synthesized by chemical vapor deposition (CVD) method (and used in this study) have shown the superior sensitivity of fM level.[6] Highly specific

detection of biomolecules with relatively small electrical charges, such as DNA or RNA molecules, has been demonstrated recently.[9] Significantly, this study did not need any PCR-based or other amplification of the analytes. An important advantage of using an electrical signal-based DNA sensor compared to existing fluorescence-based techniques is its compact size and portability. Moreover, these electronic sensors can be integrated seamlessly with wireless platforms for transmitting signals to a portable computing and/or display device such as a smart phone.Moreover, the large-scale production of graphene by CVD enables scalable production of high-quality graphene FET-based biosensors. Thus electrical signal-based DNA sensors would facilitate end-users access to DNA, RNA and other nucleic acids detection chip technology.[10]

Detection of SNP mutations with high specificity and sensitivity is essential for a broad range of diagnostic applications.[11] Recently, we have reported SNP detection using DNA strand displacement based-probe on graphene FET. Significantly, unlike commonly used short nucleic acid sequence in optical sensing, we were able to detect relatively long nucleic acid sequences with unprecedented specificity.[9] The detection did not require analytes amplification. The sensitivity, however was in nanomolar range. A more efficient design of the nucleic acid-sensing probe is necessary to achieve higher sensitivity as would be expected for the concentration of analytes in biological fluids.

In this manuscript, we report a new approach for detecting nucleic acid polymorphism using DNA nano-tweezer-based nucleic acid-sensing probes engineered to achieve an improved analytical performance when combined with a graphene FET chip. We also demonstrate the practical implementation of wireless transmission of the sensed electrical signal. First, the design of DNA nano-tweezer-based probes was tested and optimized for detection of SNP with fluorescently-labeled DNA nano-tweezers. Then DNA nano-tweezers without the fluorescent label was immobilized onto the graphene surface by π-π stacking and amine-amide bonding as previously reported.[9] The patterns and efficiency of immobilization of DNA nano-tweezers as well as their interactions with the targets were verified with atomic force microscopy (AFM) imaging. The detection of SNP was then carried-out with the graphene FET sensor.

The analytical performance of the graphene FET biosensor was examined by the electrical signal-based detection of the DNA strand displacement triggered by target DNA that drove the strand displacement and opening of the DNA nano-tweezers on the chip. When the DNA nano-tweezers open following the interactions with the target, it causes the switching of varied lengths of strands and this in turns causes a charge difference before and after strand displacement which doesn’t require any labeling or additional processes. This result changes in the measured resistance and Dirac-point of the graphene (Scheme 1). To implement wireless capabilities, the graphene DNA chip was connected to a wireless system using a microcontroller board. The analytical performance of the integrated wireless biosensor platform is validated by showing that electrical signals (e.g., current and voltage) are reliably received using wireless communication to personal electronic devices, laptops, and smartphones, for further analysis and reporting.

The scheme of strand displacement and single mismatch detection by double-stranded (DS) probe (also called zipper) and tweezers are shown in Scheme 1. The DS probe design (Scheme 1A) was successfully used previously.[9] DNA nano-tweezers are prepared by the hybridization of two complementary strands. Both normal (N) and weak strands (W) are 57 nt (Scheme 1B). N and W consisted of DS zipper, loop and hinge parts. The zipper and hinge parts are complementary, hybridized with each other while the loop parts are non-complementary, and remained un-hybridized. Therefore, N and W are complementary to each other except 10 nt of loop part in the middle of the DNA nano-tweezers. The four-guanine bases of W were substituted with inosines (I) to lessen the affinity between the two strands with respect to target strand (T). The structure of the DNA nano-tweezers with specific sequences is shown in Figure S1. As shown in Scheme 1B, when 30 nt of target strand (T), which is fully complementary with N and 5nt of the loop part on N, is introduced to DNA nano-tweezers, it displaces W and hybridizes with N. Even though the displacement happens, the hinge part is not dissociated and keeps binding with the DNA nano-tweezers; as such, the triple-stranded complex is formed.[12] Inosine (I) plays the role of shortening the toehold part. The single mismatch between T strand and N strand, significantly decrease the affinity as well as the rate of reaction compared to the perfectly matched T and N strands (Scheme 1C). This is consistent with the previous report on DNA zippers.[9]

Strand displacement was monitored over time with fluorescence labeling using Texas Red at the end of W strand (Figure 1) and a fluorescence quencher at the end of N strand. When the quencher strand (N) hybridized with the fluorescent strand (W), the fluorescence emission was quenched. In the present study, all possible variations of nucleobase (A, T, G, and C) in T strand and N strand were tested by fluorescence-based strand displacement experiment. Then one sequence was selected and tested for the following tests (Figure 1C and Figure 1D). When the T strand containing perfectly match base was added to the sample, strand displacement and the resulting higher fluorescence intensity with respect to mismatch T strand was observed (Figure 1C). The reaction kinetic analysis with respect to time clearly showed that the rate of W strand displacement with mismatch T strand was slower as well as measured fluorescence signals were lower compared to those with a perfect match T. The displacement kinetic of different T strand was evaluated by plotting heat map, which clearly showed the variation in affinity with different T strand and N strand used in the experiment (Figure 1D). The heat map analysis strongly supports the likelihood that the SNP detection and discrimination platform is suitable for genotyping.

The abovementioned results clearly show that the sensitivity and strand displacement efficiency of the DNA tweezers depend on the initial binding affinity of N-W complex as well as the binding affinity of the newly formed T-N-W complex. In this case, the T-N strands binding affinity is the deterministic factor. The perfectly matched T strand (with base T) is most likely to compete with W strand for binding with N. In other cases when N is mismatched, the affinity of N-W strands complex will also influence the sensitivity of the device. Therefore different binding kinetics (Figure 1C) and the variation in plotted heat map with the variation in A,T,C, and G (Figure 1D) were observed. The formation and operation of the DNA nano-tweezers with perfect match T and single mismatch T strands were also supported by DNA gel electrophoresis in the previous report.[9] Significantly, it should be noted that the mismatch tested in our experiments is associated with prostate cancer,

autoimmune diseases, and other common human disorders. This SNP is designated ‘rs2670660’ and biologically active non-coding RNA molecules harboring distinct SNP sequences were isolated and characterized.[13]

In order to enable electrical sensing of DNA using DNA nano-tweezers-based probes, a graphene FET with two electrodes and a liquid gate chamber was fabricated (Scheme 1C). The toehold part of N, adjacent to the graphene surface (located in the loop part, blue dotted circle), became double-stranded after the opening of DNA nano-tweezers by the strand displacement reaction (Scheme 1B). This reaction changed the electrical resistance of graphene channel as indicated in the I-V curve. DNA strand displacement-based probe namely, double stranded probe (DS probe) was reported to enhance the specificity of the DNA detection.[9] Importantly, unlike the DS probe, DNA nano-tweezers-based probe has a complex structure with the center of the probe attached to the graphene surface. As the center of the tweezers is bound on the surface, the formation of the tweezers would be V-shaped and can be hanging above the surface of the graphene (Scheme 1B). When the zipper part of the tweezer opens, the branched geometry of the triple-stranded state following interactions with the target would acquire more horizontal position. As such the target causes DNA nano-tweezers to change the DNA geometry on the graphene surface and lay down closer to the graphene plane. In effect, this conformation places the negatively charged DNA strands in a proximity to the graphene layer and hence allows more efficient interference with the electrical current.

These results support the notion that the triple stranded structure pushes the detecting portion closer to the surface resulting in a signal, which is significantly larger than what was observed previously for the DS probe. A comparison of these two different probes is described in Scheme 1A and Scheme 1B. The effective Debye length for DNA tweezer decreased compared to DS probe published earlier.[9] Thus, the reduced distance between graphene and the sensing part of “V” shaped DNA tweezer increases its sensitivity and the subsequent shift in Dirac point. We reason that this is due to the horizontal laying down formation of the DNA nano-tweezers probe (Scheme 1), while the previous DS probe remains vertically standing up.

Graphene chip fabrication and the probe immobilization were obtained by the previously published successful methods;[9] further details are provided in the methods section. The presence of graphene layers after the transfer on the silicon wafer to obtain the graphene chip was characterized by Raman microscopy. The Raman spectrum of the graphene sample indicated high-quality monolayer graphene (Figure 2A).[14] Structural features of the functionalized graphene surface were imaged by Atomic Force Microscopy (AFM). The graphene in Figure 2B shows a flat surface with some wrinkles of about 1–2 nm in height. These wrinkles are actually characteristic to the transferred graphene prepared with CVD. [15] The DNA nano-tweezers when immobilized on the graphene surface appear as globular structures with an average height of 3.7 ± 0.7 nm (Figure 2C) and are in good agreement with previously published data.[9] The DNA nano-tweezers stand up in a fluid medium (Scheme 1B) but lie down horizontally in the air (Figure 2E). An AFM image of the graphene without DNA nano-tweezers in the air is shown in Figure S2. After addition of the perfect match DNA, the height of the globular structures decreases slightly to 3.5 ± 0.8 nm,

but the diameter increases somewhat more significantly, from 17.6 ± 3.3 nm for the unbound probe to 21.8 ± 5.0 nm for the probe with the perfect match DNA (Figure 2D). AFM analysis did not show significant difference in the structure and the diameter of the unbound and bound probes. The reason might be the formation of laid down geometry by "V" shaped DNA nano-tweezers with perfect matched DNA. The binding of the perfect match DNA strand could be confirmed by AFM. The results indicate that the graphene on the fabricated FET sensor chip exists as a monolayer and supports the functionalization strategy for the complex design of DNA nano-tweezers.

The DNA strand displacement by T strand and the subsequent charge transfer showed that first few displacement events would have contributed to the effective charge transfer on the graphene surface.[16] The addition of T strand and displacement of sensing part of DNA tweezer (W strand) creates laid down geometry on the graphene surface and enables effective detection with few T strands. Moreover, the loop part of the DNA nano-tweezers that is fixed to the graphene surface facilitates the strand displacement reaction.

To examine the specificity of the graphene FET sensor, perfect match and single-mismatch samples were tested. Target strands were incubated on the graphene FET sensor overnight, the strand concentrations varied from 100 pM to 100 μM, (Figure 3). The hybridization of perfect-match sequence (T) on the graphene sensor showed left and downward shift in U-shaped I-V curve. This shift is indicative of the increasing resistance and imposition of the n-doping effect.[9] As the concentration of target strands increased, DNA tweezers showed clear discrimination of single mismatch (Figure 3A and Figure 3C). The I-V curve kept shifting left and down with increasing the concentration of perfect match (T). Significantly, 1000 times higher concentrations of single-mismatch T samples were treated on the chip and approximately only −2 mV was shifted for both 100 nM and 10 μM of single-mismatch T (Figure 3B and Figure 3C).

Nano-tweezers probes provided greater than 1000-fold improvement in sensitivity (Figure 3C) compared to the sensitivity when using a double-stranded DNA-zipper probe in the earlier study.[9] The Dirac point of the I-V curve was shifted by approximately −40 mV with 100 pM and −110 mV with 100 nM of perfect-match T, respectively. In comparison, 10 μM of target DNA was needed for a similar −40 mV shift when using the double-stranded DNA zipper as reported previously.[9] Moreover, the maximum Dirac point shift was ~110 mV with DNA tweezers while it was only ~50 mV with the previous DNA zipper probe design.[9] We reason that this is due to the transition of DNA nano-tweezers probe from vertical to horizontal formation triggered by the interactions with the target (Scheme 1). As mentioned previously, we also realized that high quality graphene grown in a defined condition would have also played an important role in improving the sensitivity from pM to fM level.[6] The single-mismatch T strand showed a much smaller shift.[9] It is reasonable to believe that a single-mismatch T strand could reduce the affinity and the proper strand displacement; however, a perfect-match T strand could increase the affinity and induce a more efficient strand displacement.

The effect of random DNA (control) on the specificity and sensitivity was examined using 32-nucleotides of a random sequence of DNA (Table S1). Random DNA was mixed in 1:1

ratio with T strands and applied to the chip. The results show that background DNA does not affect the performance of the sensor and the sensor retains the ability to discriminate against the single mismatch target (Figure 3D).

In order to determine the possibility of remote transmission of the sensed signals, wireless communication of the different sets of signals were recorded by smartphone. These recorded measurements were compared with data recorded directly with a regular multimeter. Data from the two measurement systems were well matched with only ~ 5% differences. A flow chart of the top-level design of graphene chips communication with the smartphone is presented in Figure 3F with different operation aspects highlighted by a color code (Blue: Communication, Red: Signal Generation, Black: Measurement). The details of the low-level design are presented in Figure S3. The microcontroller board was a Freescale FRDM-KL25Z with serial support, I2C, and UART communication protocols. It also provides Pulse-Width-Modulation (PWM) signal output and Analog-to-Digital Converter (ADC) allowing the board to generate and read analog signals. The setup process for the wireless signalling is further described in the following sections. The screenshot of the data received by smartphone is shown in Figure 3E. The fractional resistance change was measured for the perfect-match and the single-mismatch targets at different concentrations (Figure 3G). The accumulation of DNA on the graphene surface increased its resistance, which is supported by a significantly higher resistance of perfect-match T than single-mismatch T (Figure 3C). Clear differences were observed at all the target concentrations ranging from 100 nM to 100 μM, and it shows much clearer discrimination of the single mismatch when compared to previous work.[9] The FRDM-KL25Z microcontroller board can generate a digital approximation of an analog signal using pulse-width-modulation (PWM). The digital nature of PWM introduces noise to the system and has been determined to cause electrolysis of the aqueous electrolytes, affecting the measurements obtained. Resistances of graphene FET, with and without DNA vary by only 5%, from 3.8 kΩ to 4 kΩ. To mitigate this effect, an RC filter is used to smooth out the PWM signal. This smoothening effect reduces the peak voltage experienced by the graphene FET from 3.3 V to 0.14 V. Resistance to DNA attached graphene FET was then measured and illustrated in Figure S4A where resistance changed by 22 % from 15 kΩ to 18.3 kΩ. The results suggest that the aqueous electrolyte system and DNA attached to the graphene surface is stable. Details on how PWM causes electrolysis and how the RC filter is constructed can be found in Supporting Materials.

We used the FRDM-KL25Z microcontroller board which provides 5 analog-to-digital converters (ADC) to measure analog signals. However, the board can only measure voltages, requiring currents to be converted into voltage signals. These measurements were then plotted on an I-V graph with the gradient of the trend line representing the resistance of the entire circuit. The use of a trend line rejects measurement noise and reduces the impact of anomalous data points.

In addition, to reduce noise in the voltage measurement by the FRDM-KL25Z microcontroller board, every data point was taken as an average over 10000 measurements. Raw data points, without averaging, were used to calculate standard deviation to provide an estimate of the noise (Figure S4B). To further improve the measurement accuracy, a 2nd order moving average filter was implemented using the equation presented in supporting

materials.[17] Additional filtering further improved the measured values with minor inaccuracies (+0.35 %).

Using the wireless setup, the data was transferred to both personal computer and smartphone. The example of the screenshot is shown in Figure 3E and Figure S5. Electrical detection of a biomolecule can substitute the current fluorescence-based microarray, which would lead to better accessibility to patients. It also can contribute to end-user-friendly platforms such as a wearable or implantable biosensor. For those purposes, enhancement of specificity and wireless communication capability addressed in this paper are essential.

The further development and implementation of the technology would allow more affordable and accurate diagnosis of diseases including degenerative diseases, genetic, cancer, and other various SNP disorders[18] by an expert for effective personalized medicine. The presence of marker SNP[19] in plasma circulating DNA[20] and pM sensitivity for SNP discrimination in the unamplified sample will provide early diagnosis of disease. Our FET based SNP detection system would provide the means of real-time SNPs detection in various types of nucleic acid molecules, such as the detection of somatic mutations in Alzheimer's disease and Age-Related Macular Degeneration,[21] and SNPs associated with HIV drug resistance (HIVDR) mutations for faster antiretroviral therapy (ART).[22]

For the first time, we are reporting the high-sensitivity genotyping platform with real-time wireless capturing and transmission of the SNP detection signal. We have also minimized the non-specific binding by passivating the surface with PASE and ethanolamine, which has been shown to provide high resistance to non-cognate materials. This work contributes to the practicality of electrical-based (label-free) nucleic acid sensors by improving the portability of the sensor and the accessibility between nano-devices monitoring biomolecular nano-systems with end-user electronic devices. It will facilitate the development of digital and wireless biosensors for continuing health status monitoring, early detection and real-time therapy efficacy evaluation of life threatening human diseases. For example, in clinical applications, both SNP and single nucleotide variations (SNV), which are mechanistically linked to the individuals' somatic mosaicism would benefit from our wireless design. Wireless transmission of data will reduce the gap between patients and doctors and the device portability will promote remote medical treatment as well as minimize infections commonly associated with invasive diagnosis. Patients will be freed from the constraint of wired facilities, would have comfortable testing experience and minimized impact on their normal activities.

Supplementary Material

Refer to Web version on PubMed Central for supplementary material.

Acknowledgements

M. T. Hwang, Z. Wang, J. Ping and D. K. Ban contributed equally to this work. The work is supported by grants from National Institute on Drug Abuse R01DA024871 and 4R01AG028709–10 and departmental development funds from the Dept. of Mechanical and Aerospace Engineering, UCSD. J.P. and A.T.C.J. acknowledge support from 1P30 ES013508 from the National Institute of Environmental Health Sciences, NIH. C.F. thanks the support from the National Key R&D Program of China (2016YFA0201200, 2016YFA0400900).

REFERENCES

[1]. Barany F, Proc. Natl. Acad. Sci. U. S. A 1991, 88, 189. [PubMed: 1986365]

[2]. Jin L, Chakraborty R, Heredity 1995, 74, 274. [PubMed: 7706114]

[3]. Wang J, Rivas G, Cai X, Palecek E, Nielsen P, Shiraishi H, Dontha N, Luo D, Parrado C, Chicharro M, Farias PAM, Valera FS, Grant DH, Ozsoz M, Flair MN, Anal. Chim. Acta 1997, 347, 1.

[4]. Pei H, Lu N, Wen Y, Song S, Liu Y, Yan H, Fan C, Adv. Mater 2010, 22, 4754. [PubMed: 20839255]

[5]. Lu N, Gao A, Dai P, Song S, Fan C, Wang Y, Li T, Small 2014, 10, 2022. [PubMed: 24574202]

[6]. Ping J, Vishnubhotla R, Vrudhula A, Johnson ATC, ACS Nano 2016, 10, 8700. [PubMed: 27532480]

[7] a). Banerjee S, Wilson J, Shim J, Shankla M, Corbin EA, Aksimentiev A, Bashir R, Adv. Funct. Mater 2015, 25, 936 [PubMed: 26167144] b) He S, Song B, Li D, Zhu C, Qi W, Wen Y, Wang L, Song S, Fang H, Fan C, Adv. Funct. Mater 2010, 20, 453c) Wang Y, Li Z, Weber TJ, Hu D, Lin C-T, Li J, Lin Y, Anal. Chem 2013, 85, 6775 [PubMed: 23758346] d) Wang Y, Tang L, Li Z, Lin Y, Li J, Nat. Protoc 2014, 9, 1944. [PubMed: 25058642] e)Tang L, Wang Y, Li J, Chem. Soc. Rev, 2015, 44, 6954. [PubMed: 26144837]

[8]. Mannoor MS, Tao H, Clayton JD, Sengupta A, Kaplan DL, Naik RR, Verma N, Omenetto FG, McAlpine MC, Nat. Commun 2012, 3, 763. [PubMed: 22453836]

[9]. Hwang MT, Landon PB, Lee J, Choi D, Mo AH, Glinsky G, Lal R, Proc. Natl. Acad. Sci. U. S. A 2016, 113, 7088. [PubMed: 27298347]

[10]. Jafari HM, Abdelhalim K, Soleymani L, Sargent EH, Kelley SO, Genov R, IEEE J. Solid-State Circuits 2014, 49, 1223.

[11]. Zhang Z, Zeng D, Ma H, Feng G, Hu J, He L, Li C, Fan C, Small 2010, 6, 1854. [PubMed: 20715076]

[12] a). Landon PB, Lee J, Hwang MT, Mo AH, Zhang C, Neuberger A, Meckes B, Gutierrez JJ, Glinsky G, Lal R, Langmuir 2014, 30, 14073 [PubMed: 25347360] b)Landon PB, Ramachandran S, Gillman, Gidron T, Yoon D, Lal R, Langmuir 2012, 28, 534 [PubMed: 21875130] c) Mo AH, Landon PB, Meckes B, Yang MM, Glinsky GV, Lal R, Nanoscale 2014, 6, 1462 [PubMed: 24317092] d) Hwang MT, Landon PB, Lee J, Mo A, Meckes B, Glinsky G, Lal R, Nanoscale 2015, 7, 17397. [PubMed: 26439640]

[13] a). Glinskii AB, Ma J, Ma S, Grant D, Lim C-U, Sell S, Glinsky G, Cell Cycle 2009, 8, 3925 [PubMed: 19923886] b) Glinskii AB, Ma S, Ma J, Grant D, Lim C-U, Guest I, Sell S, Buttyan R, Glinsky GV, Cell Cycle 2011, 10, 3571. [PubMed: 22067658]

[14]. Stolyarova E, Rim KT, Ryu S, Maultzsch J, Kim P, Brus LE, Heinz TF, Hybertsen MS, Flynn GW, Proc. Natl. Acad. Sci. U. S. A 2007, 104, 9209. [PubMed: 17517635]

[15]. Ping J, Fuhrer MS, J. Appl. Phys 2014, 116, 044303.

[16]. Zhang G-J, Zhang G, Chua JH, Chee R-E, Wong EH, Agarwal A, Buddharaju KD, Singh N, Gao Z, Balasubramanian N, Nano Lett. 2008, 8, 1066. [PubMed: 18311939]

[17]. Box GE, Jenkins GM, Reinsel GC, Ljung GM, Time series analysis: forecasting and control, John Wiley & Sons, 2015.

[18] a). Harold D, Abraham R, Hollingworth P, Sims R, Gerrish A, Hamshere ML, Pahwa JS, Moskvina V, Dowzell K, Williams A, Jones N, Thomas C, Stretton A, Morgan AR, Lovestone S, Powell J, Proitsi P, Lupton MK, Brayne C, Rubinsztein DC, Gill M, Lawlor B, Lynch A, Morgan K, Brown KS, Passmore PA, Craig D, McGuinness B, Todd S, Holmes C, Mann D, Smith AD, Love S, Kehoe PG, Hardy J, Mead S, Fox N, Rossor M, Collinge J, Maier W, Jessen F, Schurmann B, Heun R, van den Bussche H, Heuser I, Kornhuber J, Wiltfang J, Dichgans M, Frolich L, Hampel H, Hull M, Rujescu D, Goate AM, Kauwe JSK, Cruchaga C, Nowotny P, Morris JC, Mayo K, Sleegers K, Bettens K, Engelborghs S, De Deyn PP, Van Broeckhoven C, Livingston G, Bass NJ, Gurling H, McQuillin A, Gwilliam R, Deloukas P, Al-Chalabi A, Shaw CE, Tsolaki M, Singleton AB, Guerreiro R, Muhleisen TW, Nothen MM, Moebus S, Jockel K-H, Klopp N, Wichmann HE, Carrasquillo MM, Pankratz VS, Younkin SG, Holmans PA, O'Donovan M, Owen MJ, Williams J, Nat. Genet 2009, 41, 1088. [PubMed: 19734902] b) Lambert J-C,

Ibrahim-Verbaas CA, Harold D, Naj AC, Sims R, Bellenguez C, Jun G, DeStefano AL, Bis JC, Beecham GW, Grenier-Boley B, Russo G, Thornton-Wells TA, Jones N, Smith AV, Chouraki V, Thomas C, Ikram MA, Zelenika D, Vardarajan BN, Kamatani Y, Lin C-F, Gerrish A, Schmidt H, Kunkle B, Dunstan ML, Ruiz A, Bihoreau M-T, Choi S-H, Reitz C, Pasquier F, Hollingworth P, Ramirez A, Hanon O, Fitzpatrick AL, Buxbaum JD, Campion D, Crane PK, Baldwin C, Becker T, Gudnason V, Cruchaga C, Craig D, Amin N, Berr C, Lopez OL, De Jager PL, Deramecourt V, Johnston JA, Evans D, Lovestone S, Letenneur L, Morón FJ, Rubinsztein DC, Eiriksdottir G, Sleegers K, Goate AM, Fiévet N, Huentelman MJ, Gill M, Brown K, Kamboh MI, Keller L, Barberger-Gateau P, McGuinness B, Larson EB, Green R, Myers AJ, Dufouil C, Todd S, Wallon D, Love S, Rogaeva E, Gallacher J, St George-Hyslop P, Clarimon J, Lleo A, Bayer A, Tsuang DW, Yu L, Tsolaki M, Bossù P, Spalletta G, Proitsi P, Collinge J, Sorbi S, Sanchez-Garcia F, Fox NC, Hardy J, Deniz Naranjo MC, Bosco P, Clarke R, Brayne C, Galimberti D, Mancuso M, Matthews F, I. European Alzheimer's disease, Genetic, D. Environmental Risk in Alzheimer's, C. Alzheimer's Disease Genetic, H. Cohorts for, E. Aging Research in Genomic, Moebus S, Mecocci P, Zompo MD, Maier W, Hampel H, Pilotto A, Bullido M, Panza F, Caffarra P, Nacmias B, Gilbert JR, Mayhaus M, Lannfelt L, Hakonarson H, Pichler S, Carrasquillo MM, Ingelsson M, Beekly D, Alvarez V, Zou F, Valladares O, Younkin SG, Coto E, Hamilton-Nelson KL, Gu W, Razquin C, Pastor P, Mateo I, Owen MJ, Faber KM, Jonsson PV, Combarros O, O'Donovan MC, Cantwell LB, Soininen H, Blacker D, Mead S, Mosley TH, Bennett DA, Harris TB, Fratiglioni L, Holmes C, de Bruijn RFAG, Passmore P, Montine TJ, Bettens K, Rotter JI, Brice A, Morgan K, Foroud TM, Kukull WA, Hannequin D, Powell JF, Nalls MA, Ritchie K, Lunetta KL, Kauwe JSK, Boerwinkle E, Riemenschneider M, Boada M, Hiltunen M, Martin ER, Schmidt R, Rujescu D, Wang L.-s., Dartigues J-F, Mayeux R, Tzourio C, Hofman A, Nöthen MM, Graff C, Psaty BM, Jones L, Haines JL, Holmans PA, Lathrop M, Pericak-Vance MA, Launer LJ, Farrer LA, van Duijn CM, Van Broeckhoven C, Moskvina V, Seshadri S, Williams J, Schellenberg GD, Amouyel P, Nat. Genet 2013, 45, 1452. [PubMed: 24162737] c) Simon-Sanchez J, Scholz S, del Mar Matarin M, Fung H-C, Hernandez D, Gibbs JR, Britton A, Hardy J, Singleton A, Hum. Mutat 2008, 29, 315. [PubMed: 17994548] d) Gaylord BS, Massie MR, Feinstein SC, Bazan GC, Proc. Natl. Acad. Sci. U. S. A 2005, 102, 34. [PubMed: 15618399] e) Gough SCL, Walker LSK, Sansom DM, Immunol. Rev. 2005, 204, 102. [PubMed: 15790353] f) Mori M, Yamada R, Kobayashi K, Kawaida R, Yamamoto K, J. Hum. Genet 2005, 50, 264. [PubMed: 15883854] g) Liu X, Kawamura Y, Shimada T, Otowa T, Koishi S, Sugiyama T, Nishida H, Hashimoto O, Nakagami R, Tochigi M, Umekage T, Kano Y, Miyagawa T, Kato N, Tokunaga K, Sasaki T, J. Hum. Genet 2010, 55, 137. [PubMed: 20094064] h) Klein RJ, Zeiss C, Chew EY, Tsai J-Y, Sackler RS, Haynes C, Henning AK, SanGiovanni JP, Mane SM, Mayne ST, Bracken MB, Ferris FL, Ott J, Barnstable C, Hoh J, Science 2005, 308, 385. [PubMed: 15761122]

[19]. Sachidanandam R, Weissman D, Schmidt SC, Kakol JM, Stein LD, Marth G, Sherry S, Mullikin JC, Mortimore BJ, Willey DL, Hunt SE, Cole CG, Coggill PC, Rice CM, Ning Z, Rogers J, Bentley DR, Kwok PY, Mardis ER, Yeh RT, Schultz B, Cook L, Davenport R, Dante M, Fulton L, Hillier L, Waterston RH, McPherson JD, Gilman B, Schaffner S, Van Etten WJ, Reich D, Higgins J, Daly MJ, Blumenstiel B, Baldwin J, Stange-Thomann N, Zody MC, Linton L, Lander ES, Altshuler D, Nature 2001, 409, 928. [PubMed: 11237013]

[20] a). Elshimali YI, Khaddour H, Sarkissyan M, Wu Y, Vadgama JV, Int. J. Mol. Sci 2013, 14, 18925. [PubMed: 24065096] Thierry AR, Mouliere F, Gongora C, Ollier J, Robert B, Ychou M, Del Rio M, Molina F, Nucleic Acids Res. 2010, 38, 6159. [PubMed: 20494973]

[21] a). Regan W, Alem N, Alemán B, Geng B, Girit Ç, Maserati L, Wang F, Crommie M, Zettl A, Appl. Phys. Lett 2010, 96, 113102.b) Sedra AS, Smith KC, Microelectronic Circuits: International edition, OUP USA, 2010.c) Barr M, Embedded Systems Programming, 14, 103.

[22]. T. I. S. S. Group, N. Engl. J. Med 2015, 373, 795. [PubMed: 26192873]

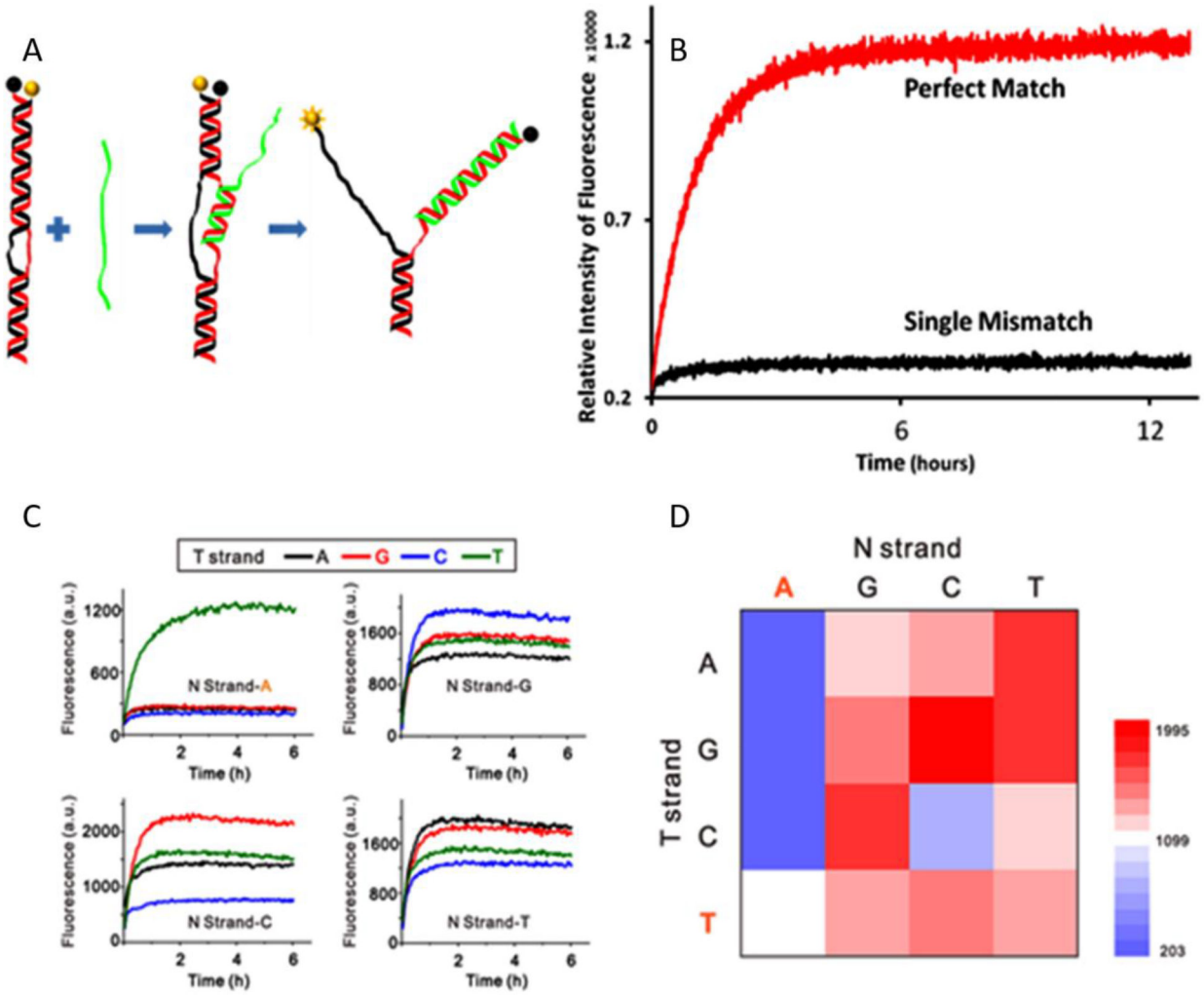

Figure 1.

Single-mismatch detection using fluorescently labeled DNA tweezers. (A) Schematics of strand displacement: the W strand (black with fluorophores labeled in yellow) and N strand (red with quencher labeled as black ball) were hybridized to form DNA tweezers. When the perfect-match T strand (green) interacts with DNA tweezers, the displacement of W strand by T activates the fluorophore. (B) The kinetics of strand displacement was measured by time dependent fluorescence measurement. The single-mismatch target strand interaction with DNA tweezers show less fluorescence activity compared to the interaction of the perfect match with DNA tweezers. (C) Real-time fluorescence measurement of the strand displacement. The DNA tweezers with the original N strand show high selectivity towards the perfect match T strand. The fluorescence intensity of DNA tweezers with single mismatch N strand is in positive correlation with the bonding strength between the base pairs in different combination (analyzed with NUPACK). (D) Heat Map depicting the fluorescence recovery of Texas Red labeled on W strand after the addition of T strand at 6 h. The perfect match is labeled in orange.

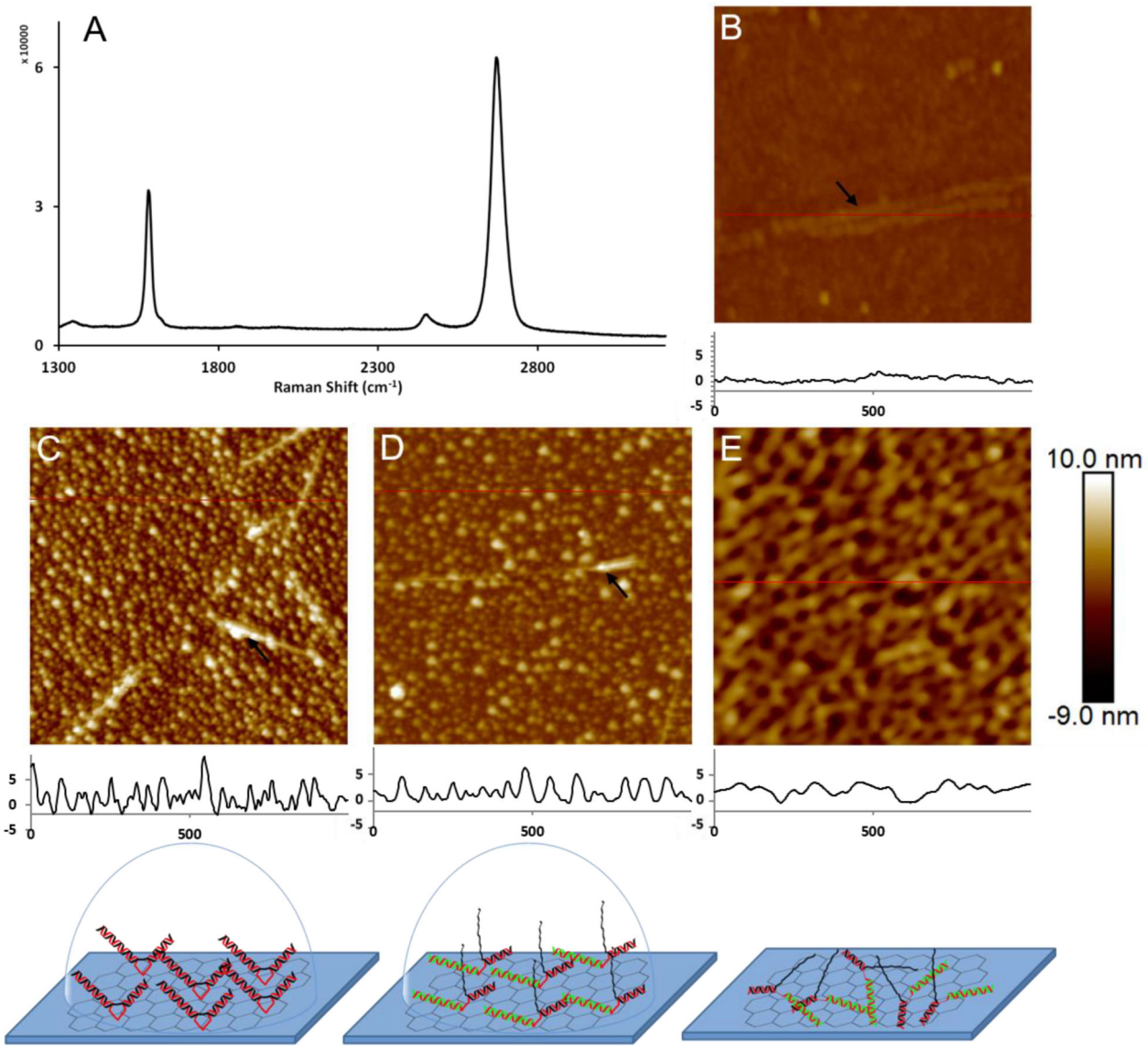

Figure 2.

Raman spectrum analysis of graphene surface and AFM images of graphene transistor surface with and without the DNA sensor. A) Raman spectrum of the CVD graphene confirm that the transferred graphene was a single layer. B) AFM imaging of graphene surface in fluid showed mostly flat surface with some wrinkles. C) Graphene surface covered with DNA tweezers in fluid. The strands produce features of ~2–8 nm in height with an average diameter of about 18 nm. D) The binding of a perfect match DNA strand in fluid causes decrease in height of ~2–6 nm and increase in diameter to ~22 nm. E) AFM images of graphene transistor surface with the DNA tweezers sensor linked to graphene in air was random polygonal patterns lied down on the surface was observed. Black arrows in C and D indicate wrinkles on graphene surface. Cartoons at the bottom represent models of DNA structure in liquid and air. All images have a scan area of 1 × 1 μm and the surface height profiles are in nm while “z” was in the range of 19 nm.

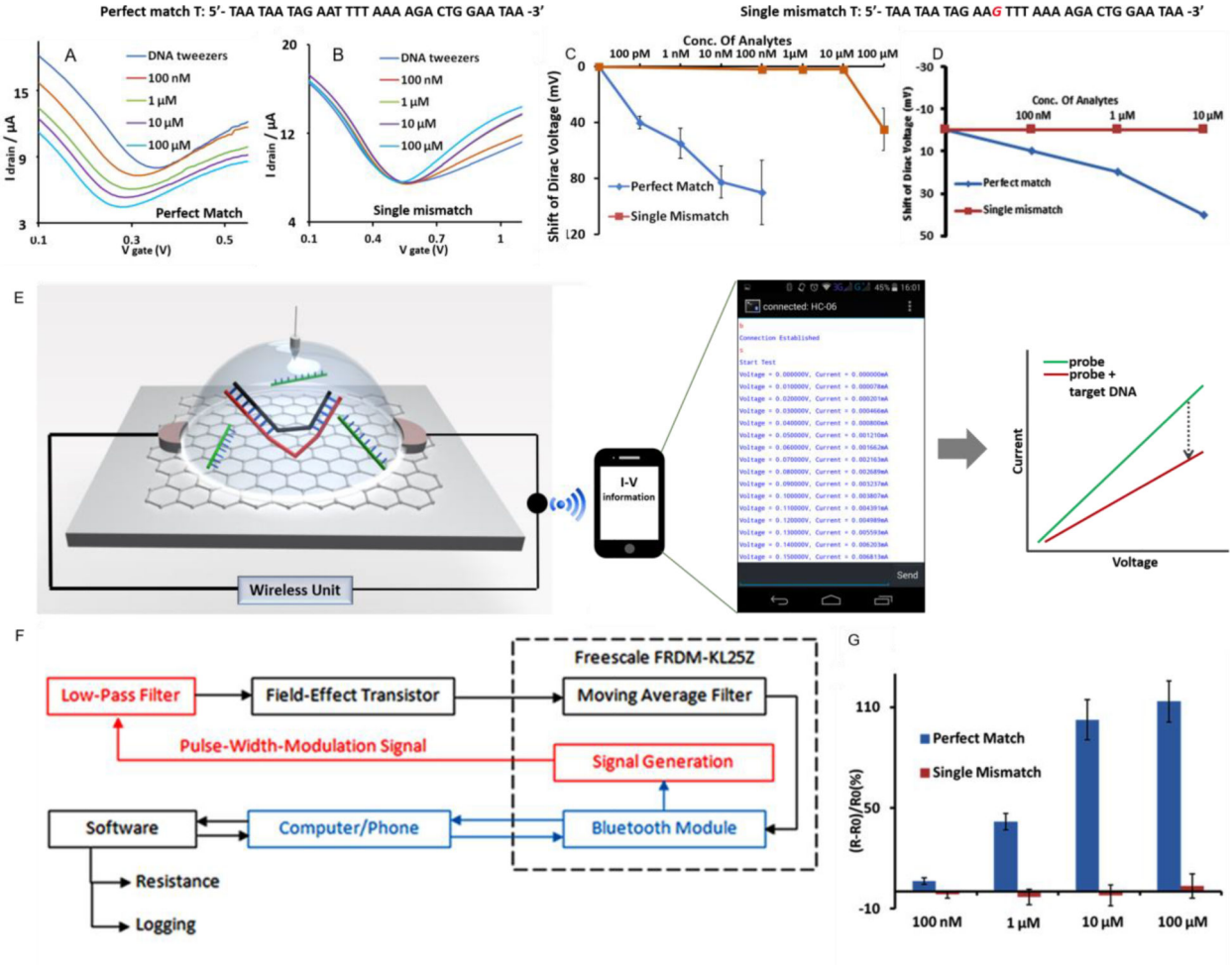

Figure 3.

The strand displacement reactions on graphene FET and I-Vg relationship of the graphene FET sensor (A to D).The working principle of the wireless data transmission device (E to G). A) The shift in I-V curve with different concentration of perfect-match T (100 pM-100 nM). B) The single-mismatch T showed significantly less shifts the I-V curve with similar concentration of T. The DNA sequences of T used in the different experiments are shown over the I-Vg curve. C) Dirac voltage shift of the FET sensor as a function of the target concentration. D) Dirac voltage shift of the FET sensor with background DNA. E) The schematics of the data transmission in wireless mode from the biosensor chip to a smartphone was shown. The resistance value was further processed using electrical voltage and current data transmitted to a smartphone. The magnified screenshot of Smartphone screen showed Bluetooth terminal mediated data received by Smartphone demonstrate communication between sensor device and Smartphone. The resistance changes before and after the detection of DNA was interpreted as I-V graph. F) Top-level design of the device with different operation modules highlighted. (Blue: Communication, Red: Signal Generation, Black: Measurement). G) The significant resistance changes of the channel layer caused by strand displacement at different concentrations of the T DNAs.

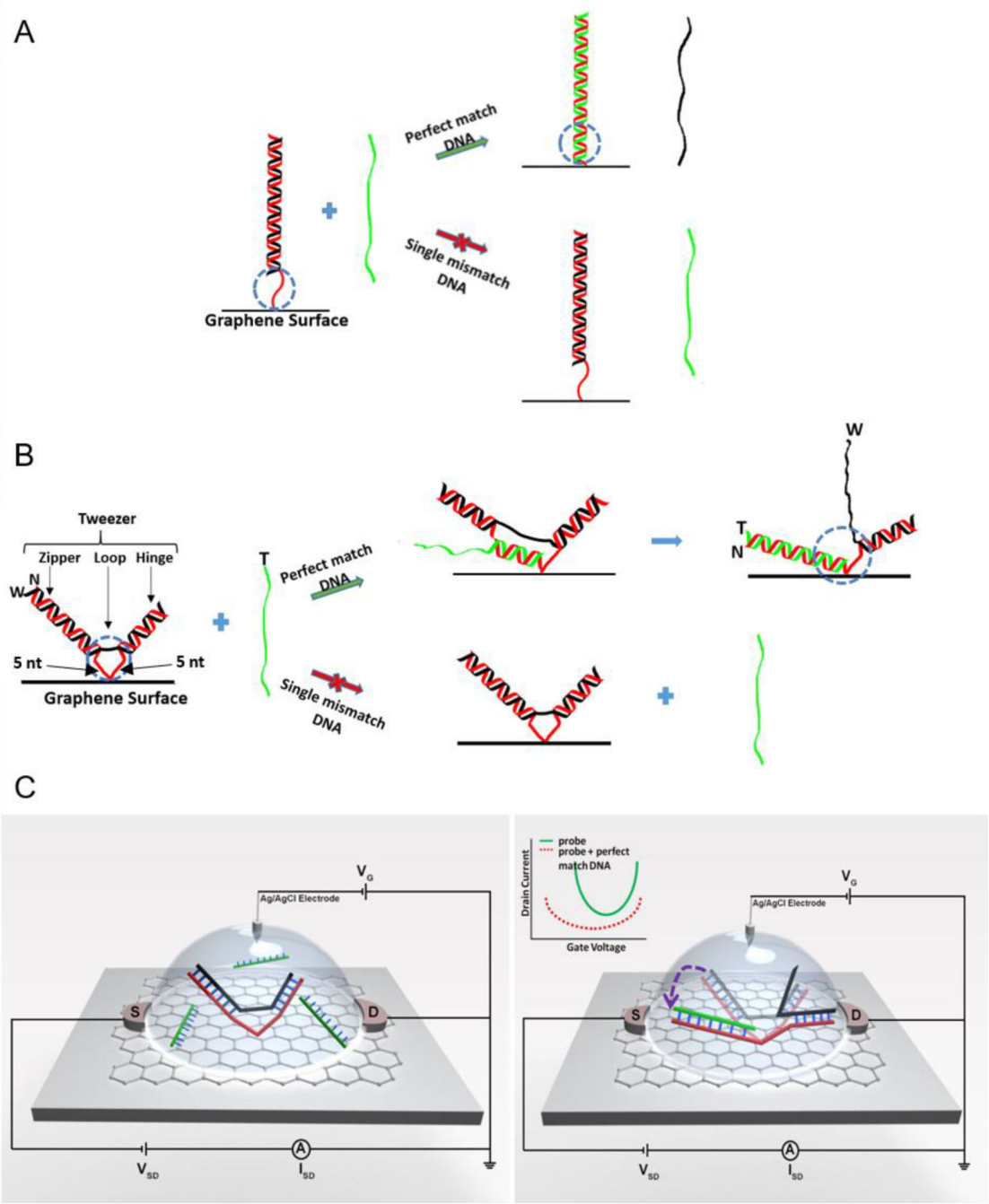

Scheme 1.

Schematics of the DNA nano-sensors. (A) Previously reported double-stranded (DS) probe design [9] stands vertically on the graphene surface. The T strand displaces the W strand, and the toehold portion becomes double-stranded, thus more charges from DNA are accumulated and detected. The electrical effect of DNA was reported to be rapidly decreased with distance, and only a few nucleotides (blue dot circle) that are close to the graphene surface influence the electrostatic potential on the sensor. (B) DNA nano-tweezers probe design. The probe was horizontally laid down on the graphene surface, placing the longer DNA sequence

of charge accumulation part (blue dot circle) in close proximity to the graphene surface. When the T strand displaces the W strand, the single-stranded toehold region becomes double-stranded, the overall probe architecture becomes triple-stranded bringing the longer DNA sequences of the charge accumulation part closer to the surface than the DS probe and gives larger signal. However single-mismatch T strand prohibits efficient strand displacement leaving the toehold region single-stranded. (C) Schematics of graphene FET sensor with DNA tweezers probe. Gate voltage was applied directly on the liquid gate (shown as a light blue hemisphere). I-V curve shifts leftwards and downwards only during the perfect match T strand displacement (The inset).